Available online at www.sciencedirect.com
SCIENCE DIRECT®
Vision Research 45 (2005) 2059–2064
Vision Research
www.elsevier.com/locate/visres

Rapid communication

Optimal size for perceiving motion decreases with contrast

Duje Tadin *, Joseph S. Lappin

Vanderbilt Vision Research Center and Department of Psychology, Vanderbilt University, 111 21st Avenue S, Nashville, TN 37203, United States

Received 2 July 2004; received in revised form 26 January 2005

Abstract

Visual patterns have widely varying contrasts and elicit local signals of varying reliability, ranging from noisy to relatively noise-free. One way to deal efficiently with the variable visual input is to employ flexible neural mechanisms that adapt to changing conditions. We investigated whether the spatial properties of motion mechanisms change with stimulus contrast and found that the optimal size for perceiving motion decreases with increasing contrast. These data were well-described by a model in which spatial summation increases with decreasing contrast.

Keywords: Motion; Center–surround interactions; Surround inhibition; Spatial summation; Area MT

1. Introduction

The bulk of our psychophysical knowledge about the spatial properties of motion mechanisms comes from threshold experiments, usually contrast or motion coherence thresholds. Several groups have described the effects of increasing stimulus size on contrast and signal/noise thresholds, and have found that thresholds first improve rapidly with increasing size, and then level off or improve at a slower rate (Anderson & Burr, 1987, 1991; Fredericksen, Verstraten, & van de Grind, 1994; Gorea, 1985; van de Grind, Koenderink, & Doorn, 1986; Lappin & Bell, 1976; Watson & Turano, 1995). The initial rapid improvement is usually attributed to spatial summation within a single neural mechanism; and gradual improvement at larger sizes indicates probability summation over multiple mechanisms. These experiments assume that the spatial properties of the underlying neural mechanisms are independent of stimulus contrast.

At the time, this contrast-invariance assumption agreed with the physiological conception of a receptive field as a fixed property of a neuron. Recent studies, however, have found that spatial properties of the receptive field are dynamic and depend on the stimulus and the visual context (Cavanaugh, Bair, & Movshon, 2002; Dragoi & Sur, 2000; Kapadia, Westheimer, & Gilbert, 1999; Levitt & Lund, 1997; Sceniak, Ringach, Hawken, & Shapley, 1999). Many of the observed changes in the receptive field physiology are believed to result from contrast-dependent interactions between excitatory and inhibitory processes. Specifically, spatial summation has been found to increase with decreasing contrast (Sceniak et al., 1999). Moreover, surround suppression often becomes more pronounced at high contrast (Cavanaugh et al., 2002). Such adaptive receptive fields make functional sense: At low contrast, sensitivity can be improved by increased spatial summation and reduced surround suppression. When visibility is well above threshold, however, spatial resolution can be improved by reducing spatial summation and taking

* Corresponding author. Tel.: +1 615 322 2398; fax: +1 615 343 8449.
E-mail address: duje.tadin@vanderbilt.edu (D. Tadin).

0042-6989/$ - see front matter © 2005 Published by Elsevier Ltd.
doi:10.1016/j.visres.2005.01.029

advantage of center–surround antagonism to differentiate spatial patterns.

These recent neurophysiological findings suggest that psychophysically described motion mechanisms may also change with contrast. Indeed, Tadin, Lappin, Gilroy, and Blake (2003) found that the "sign" of spatial interactions changes with contrast: with spatial summation at low contrast and spatial suppression at medium and high contrasts. The counterintuitive finding was that direction discriminations at high and medium contrasts were improved by reducing the size of the motion pattern. This relation between size and discrimination thresholds of high-contrast patterns should be U-shaped, however: Further reductions in size below some optimal value should yield reduced discriminations. This minimum-threshold size may be taken to indicate the size at which spatial summation and suppression are optimally balanced.

A general aim of the present study was to identify an optimal size for perceiving motion. A more specific question was whether this optimal size varies with stimulus contrast. One possibility is that the spatial areas and the relative strengths of summation and suppression are independent of contrast, resulting in a fixed optimal size. (Note that an "optimal size" concept only applies to medium and high contrasts that show significant surround suppression.) Another possibility is that the optimal size changes with contrast—possibly decreasing as contrast increases. The results of Tadin et al. (2003) do not distinguish between these two alternatives because they focused on relatively large stimulus sizes (as limited by 1 cycle/° Gabor stimuli). We investigated this question by using dense random-pixel moving stimuli and measuring duration thresholds.[1]

2. Methods

Stimulus patterns were created in MATLAB with the Psychophysics Toolbox (Brainard, 1997) and Video Toolbox (Pelli, 1997) and shown on a linearized monitor (1024×768 pixels resolution, 120 Hz). Viewing was binocular at 83 cm. The ambient illumination was 4.8 cd/m^2 and the background gray-level luminance was 60.5 cd/m^2. To allow presentation of brief motion stimuli, the contrast of a stimulus was ramped on and off with a temporal Gaussian envelope (duration was defined as two standard deviations (2σ) of the temporal Gaussian). Thresholds (82%) were estimated by interleaved Quest staircases. For each condition, observers participated in four blocks, with two interleaved staircases in each block. The first block was discarded as practice, yielding six independent thresholds estimates for each observer in each condition. All experiments complied with institutionally reviewed procedures for human subjects. Four naïve and well-practiced observers participated in the study.

The stimuli were dense random-pixel motion patterns made up of light and dark pixels (each 3.1×3.1 arcmin) presented in a spatial Gaussian envelope. Size was defined as 2σ of the spatial Gaussian. Contrast was defined as the peak contrast of the spatial Gaussian. From frame to frame of the animation, half of the pixels shifted by 3.1 arcmin in one direction (6.2 °/s) while the remaining pixels were randomly regenerated (i.e., yielding 50% correlation)—conditions producing vivid motion perception at suprathreshold exposure durations.[2]

We measured the threshold exposure duration required for observers to accurately identify the motion direction. On each trial, a moving stimulus was presented foveally and the observer indicated the perceived direction (left or right) by a key press. Feedback was provided. In separate conditions, observers viewed foveally presented random-pixel motion stimuli of eight different sizes (0.25°–6°) and four contrasts (9–92%), yielding 32 conditions.

To gain insight into the properties of putative mechanisms that may account for our results we fitted three models to the data (see Appendix A). The models were chosen because they allowed for greater spatial summation at low contrast and/or stronger inhibition at high contrast, albeit in different ways. In the *CRF Model*, different contrast response functions are used for excitatory center and inhibitory surround responses, allowing relative strengthening of inhibition with increasing contrast. The *Size Model* allowed for size of the excitatory center region to vary (i.e., decrease) with contrast (cf., Sceniak et al., 1999), thus favoring greater summation at low contrasts. Finally, in the *Drive Model*, effective strength of the inhibitory surround influence was controlled by the activation (i.e., drive) of the excitatory center mechanism (cf., Somers et al., 1998). This model ensures that, regardless of contrast, all weak excitatory responses (i.e., applying to *both* high-contrast small stimuli and low-contrast large stimuli) are not

[1] Use of duration thresholds was based on the assumption that if the neural response to a stimulus is weak and/or noisy, then longer stimulus exposure will be required for correct perception. More specifically, deciding whether an object is moving in one of two possible directions can be conceptualized as a process involving accumulation of sensory evidence over time (Gold & Shadlen, 2000; Roitman & Shadlen, 2002). When neuronal responses are noisy or attenuated, as with a highly suppressed motion stimulus, sensory evidence accumulates more slowly and a correct decision thus may require longer exposure duration (Roitman & Shadlen, 2002).

[2] We used 50% correlation to avoid floor effects that were encountered in pilot work. One subject, however, had difficulty with 50% correlation (thresholds were high and very variable), thus she completed the experiment with 100% correlated motion. Her results at 100% correlation were qualitatively identical to those of other subjects at 50% correlation, but were not included in the average data.

"erased" by surround inhibition. Goodness-of-fit was assessed with a *Chi-square* test ($df = 22$):

$$\chi^2 = \sum_i ((m_i - t_i)^2/\sigma_i^2)$$

where m_i was model's output for the ith stimulus condition, t_i was average threshold for that condition, and σ_i^2 was the between-subject variance of the threshold estimate.

3. Results

Increasing the size of a low-contrast moving stimulus resulted in improved performance, whereas the same size increase for high-contrast stimuli ultimately resulted in decreasing performance-suggesting surround suppression (Fig. 1A). This replicates the main result of Tadin et al. (2003). Furthermore, at each contrast where surround suppression was observed (20%, 42%, 92%), we observed an optimal size—an intermediate size at which the threshold was the lowest. More notably, this optimal size decreased with increasing contrast: At 92% contrast, the optimal size was half the size of that at 20% contrast (0.5° vs 1°) and no optimal size was observed at 9% contrast. This pattern of results was observed for all subjects.

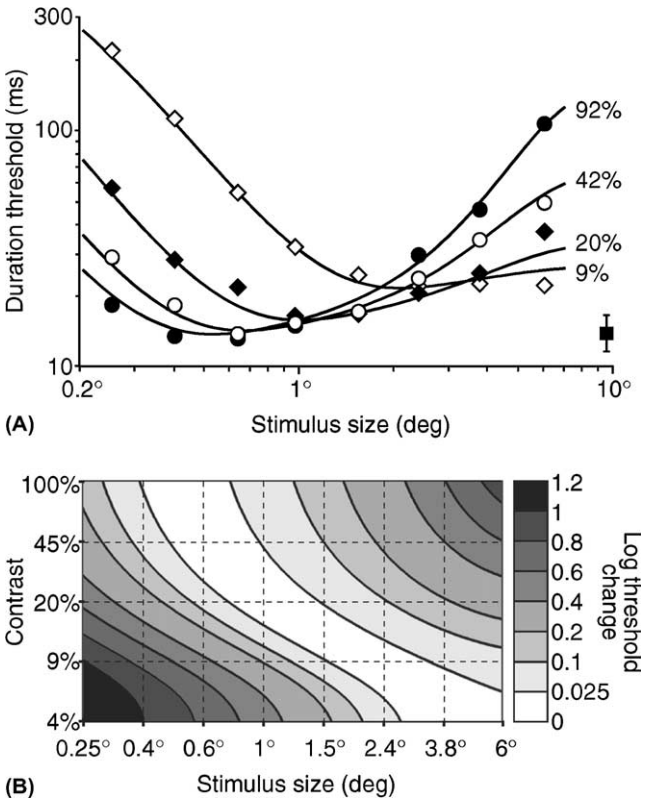

Fig. 1. Motion discriminations as a function of stimulus size at different contrasts. (A) Average duration thresholds. Fitted curves are the predictions of the *Size Model* (see Appendix A). For each contrast, the stimulus size yielding the minimum *Size Model* prediction was taken as the optimal size for that contrast. For clarity, only the average between-subject SEM of all data points is shown (filled square). (B) Log threshold change relative to the optimal size. At each contrast, predictions of the *Size Model* were normalized relative to the minimum prediction at that contrast (log threshold change = $\log(f(x)) - \log(\min(f(x)))$). The color bar on the right indicates levels of log threshold change relative to the minimum threshold (note the non-linear scale). The diagonally oriented white region indicates that the optimal size increases with decreasing contrast.

The *Size Model* provided the best fit to the data ($\chi^2 = 8.2$, $p > 0.99$) and its predictions are shown in Fig. 1. A good fit was also obtained with the *Drive Model* ($\chi^2 = 17.3$, $p > 0.75$). Visually, the *Drive Model* and *Size Model* predictions were similar, with both models yielding comparable estimates of the optimal sizes. The *Drive Model* provided a better fit for the largest sizes at 9% contrast (i.e., did not exhibit the small upward turn that is apparent in Fig. 1A), but yielded significant deviations in both directions for the largest sizes at higher contrasts (Fig. 3B). In addition, the *Size Model* yielded spatial parameters that are more realistic (see Appendix A). As defined, the *CRF Model* did not fit the data well ($\chi^2 = 113$, $p < 0.00001$). The *CRF Model* had problems reproducing the shift in the optimal size that is evident in psychophysical data (Fig. 3A). Specifically, the optimal sizes for 20%, 42% and 92% contrasts *and* the size at which 9% contrast fit started to asymptote were all between 0.7° and 0.9°.

To better visualize the contrast-dependent change in the optimal stimulus size, we plotted normalized predictions of the *Size Model* in an area graph (Fig. 1B). It is clear that the minimum threshold (white region) shifts to a smaller size as the contrast increases. Moreover, surround inhibition is evident for contrasts greater than 10%, while spatial summation dominates at lower contrasts. This "turnaround" point is larger than the 5% contrast value reported by Tadin et al. (2003)—a difference likely due to the different stimuli used (broad-band random-pixel patterns vs. Gabor patches).

Presenting the duration thresholds as a function of contrast shows that the discriminations of small moving stimuli improved with contrast, while the visibility of large stimuli counterintuitively decreased with increasing contrast (Fig. 2A). From these data, we extracted a contrast-dependency index for each size—defined as the log threshold change between the lowest and the highest contrast. Fig. 2B shows that the contrast-dependency of motion discrimination changes in a very orderly manner with increasing size: contrast has a facilitatory effect for small sizes and an inhibitory effect for large sizes. From Fig. 2B, we estimated that the intermediate size for which increasing contrast from 9% to 92% has the least effect on motion discrimination is about 2° (114 arcmin).

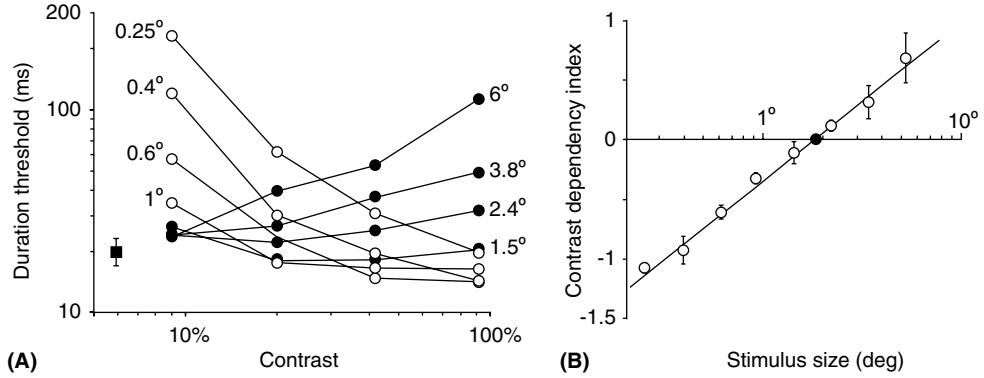

Fig. 2. Motion discriminations as a function of contrast at different stimulus sizes. (A) Average duration thresholds. Empty circles indicate stimulus sizes for which increasing contrast improves motion discriminations. Filled circles indicate stimulus sizes for which increasing contrast worsens motion discriminations. For clarity, only the average between-subject SEM of all data points is shown (filled square).(B) Contrast-dependency index. For each size, a contrast-dependency index was calculated as (log threshold at 92% contrast) − (log threshold at 9% contrast). Negative numbers indicate contrast facilitation, while positive numbers show contrast inhibition. The zero-crossing (indicated by a filled circle at about 2° size) was computed from a linear function fitted to the data ($r^2 = 0.994$). Error bars are between-subject SEM.

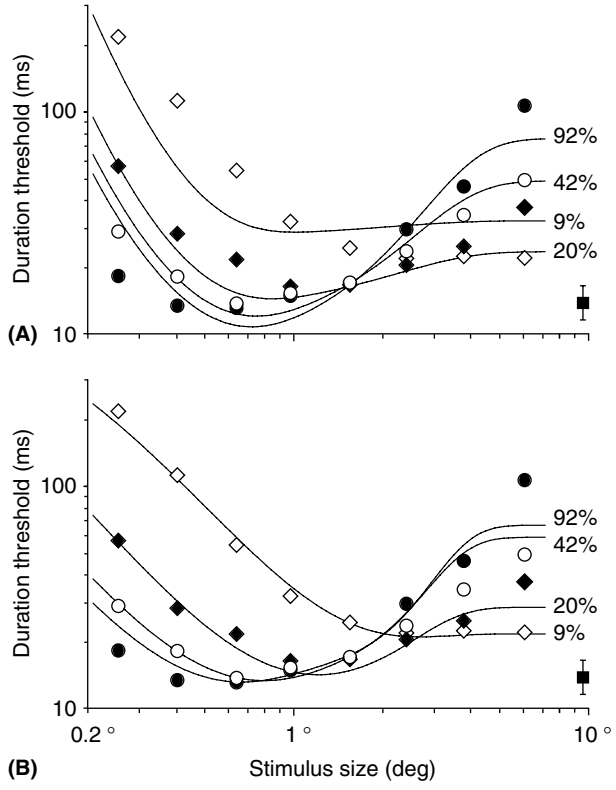

Fig. 3. Predictions of (A) the *CRF Model* and (B) the *Drive Model* fitted to the duration threshold data. For clarity, only the average between-subject SEM of all data points is shown (filled square).

4. Discussion

We show that spatial properties of motion perception depend critically on contrast. Specifically, we found that the optimal size for perceiving motion decreases (approx. twofold) with increasing contrast. This result dovetails nicely with reports indicating that the receptive field size in cortical area V1 decreases with contrast, with the magnitude of change between twofold and fourfold (Cavanaugh et al., 2002; Kapadia et al., 1999; Sceniak et al., 1999). The relatively small optimal sizes reported here (as low as 0.5°) were likely the result of the stimulus we used: broad-band motion composed of high-density small (0.05°) elements. Investigation of other moving stimuli (e.g., narrow-band motion) and stimulus parameters (e.g., spatial frequency, eccentricity) will likely yield different quantitative estimates of optimal sizes, but, we speculate, will also show analogous contrast-dependency of the optimal size.

Furthermore, our results raise warning flags about interpreting the previous studies of the receptive field properties of human motion mechanisms (Anderson & Burr, 1987, 1991; Fredericksen et al., 1994; Gorea, 1985; van de Grind et al., 1986; Lappin & Bell, 1976; Watson & Turano, 1995). Those studies provided important data about basic spatial properties of motion mechanisms operating in low visibility conditions, but such results do not generalize to conditions when visibility (i.e., contrast and signal/noise) of the stimulus is well above threshold.

We speculate that the optimal size for perceiving motion indicates a size at which the inhibitory surround mechanisms prevail over the spatial summation by the excitatory center mechanisms. The contrast dependency of this effect, then, can be accounted for by asymmetric interactions between excitatory center and inhibitory surround mechanisms. The precise nature of such asymmetry, however, is still unknown. For example, larger optimal size at low contrast may be a result of the summating center mechanisms whose spatial extent grows with decreasing contrast (Sceniak et al., 1999). In such models, increasing spatial summation at low contrast essentially swamps inhibitory surround signals that would otherwise have a strong effect on neural response.

Alternatively, a change in the receptive field size can be caused by surround mechanisms that "turn on" only at higher contrasts and/or center activations, with both center and surround being spatially fixed (Cavanaugh et al., 2002; Somers et al., 1998). The consequence of such asymmetry will be that the surround effect will remain below threshold when the center activation is low. However, as the center response increases, the inhibitory surround will gradually "erode" the spatial summation by the excitatory center. Our modeling results have shown that versions of each of these receptive field models provide good fits to the reported psychophysical measurements, with the *Size Model* yielding more realistic parameters.

All the aforementioned neurophysiological models and most other investigations of the relationship between receptive field size and contrast have been based on V1 data. Undoubtedly, it would be useful to have more results from other visual areas, especially MT given its important role in motion perception and strong surround suppression (Allman, Meizin, & McGuiness, 1985). Based on our earlier psychophysical findings, we hypothesized that the balance between surround suppression and spatial summation in MT will depend on contrast (Tadin et al., 2003). Unfortunately, nearly all published studies of surround suppression in MT were restricted to high-contrast moving stimuli. A recent study, however, demonstrated that the center–surround antagonism observed at high contrast in MT substantially weakens or even disappears at low contrast (Pack, Hunter, & Born, 2005). Thus, contrast-dependent pooling of spatially distributed motion signals, analogous to that observed in V1, is a prominent feature of neural computation in MT.

In summary, we found that the spatial integration of motion signals depends on contrast. This finding accords with observations in V1 and MT indicating that the stimulus size evoking the best response decreases with contrast. Finally, we suspect that this result is not specific to contrast, as other stimulus parameters have also been shown to affect the spatial properties of visual neurons (e.g., Ito & Gilbert, 1999; Kapadia et al., 1999; Lamme, 1995; Solomon, Peirce, & Lennie, 2004; Treue, 2001). For example, spatial properties of motion mechanisms might also adjust adaptively to changes in signal/noise ratio, chromatic properties, figure/ground belongingness, and allocated attention.

Acknowledgements

This work was supported by P30-EY08126. DT was supported by EY07760 to Randolph Blake. We thank Jason Samonds for helpful suggestions.

Appendix A

All of the tested models (Table 1) shared some basic characteristics. Model outputs were functions of both size (w) and contrast (c). Contrast response functions (CRFs) for both excitation (*ECrf*) and inhibition (*ICrf*) were modeled with a Naka–Rushton function—a model that provides a good description of neural responses across brain areas (Sclar, Maunsell, & Lennie, 1990). Spatial extents of excitation and inhibition (i.e., receptive field activations) were described with the error function (erf), which is the integral of a Gaussian (cf., Pack et al., 2005; DeAngelis & Uka, 2003). Sizes of the excitatory center and the inhibitory surround are denoted with α and β, respectively. Note that in all models, surround activation was scaled by β/α. This ensures that when outputs of $\mathrm{erf}(w/\alpha)$ and $\mathrm{erf}(w/\beta)$ are near the maximum (i.e., 1), the inhibitory surround activation remains larger by a factor of β/α than the center activation.

The response strength (R) was calculated by subtracting the inhibitory (I) from the excitatory (E) response and adding a baseline response (R_0). Threshold (T) was taken to equal the number of times a response (R) needed to be repeated to reach a certain *Criterion*—essentially modeling "how long" the response needed to be maintained in order to generate sufficient evidence about the motion direction of the stimulus. This computation models the accumulation of evidence that likely underlies duration threshold measurements (see Footnote 1). To keep models relatively simple, we assumed perfect integration of evidence, rather than a more realistic alternative that would require some type of a

Table 1
Formal description of models

	Contrast response function	Excitation and inhibition	Response computation
CRF Model	$ECrf(c) = A_e \cdot c^e/(c^e + c^e_{50e})$ $ICrf(c) = A_i \cdot c^i/(c^i + c^i_{50i})$	$E(w,c) = ECrf(c) \cdot \mathrm{erf}(w/\alpha)$ $I(w,c) = ICrf(c) \cdot \mathrm{erf}(w/\beta) \cdot (\beta/\alpha)$	$R = R_0 + E - I$ $T = \mathrm{Criterion}/R$
Size Model	$ECrf(c) = A_e \cdot c^n/(c^n + c^n_{50})$ $ICrf(c) = A_i \cdot ECrf(c)$	$\alpha(c) = S/(1 + m \cdot e^{(-k/c)})$ $E(w,c) = ECrf(c) \cdot \mathrm{erf}(w/\alpha(c))$ $I(w,c) = ICrf(c) \cdot \mathrm{erf}(w/\beta) \cdot (\beta/\alpha(c))$	$R = R_0 + E - I$ $T = \mathrm{Criterion}/R$
Drive Model	$ECrf(c) = A_e \cdot c^n/(c^n + c^n_{50})$ $ICrf(c) = A_i \cdot ECrf(c)$	$E(w,c) = ECrf(c) \cdot \mathrm{erf}(w/\alpha)$ $I(w,c) = ICrf(c) \cdot \mathrm{erf}(w/\beta) \cdot (\beta/\alpha)$ $D(x) = 1/(1 + m \cdot e^{(-x/k)})$ where $x = E(w,c)/E_{\max}$	$R = R_0 + E - I \cdot D$ $T = \mathrm{Criterion}/R$

leaky integrator. Each model had eight free parameters (in addition to scaling parameters R_0 and *Criterion*). Model fitting was performed using the least squares algorithm with MATLAB and Optimization Toolbox (Mathworks, Natick, MA). Model specific parameters and computational details are described below:

CRF Model (predictions shown in Fig. 3A): Excitation and inhibition were modeled with different CRFs. That is, the maximum amplitudes (A_e, A_i), Naka–Rushton exponents (e, i) and contrast at half-amplitude (c_{50e}, c_{50i}) were adjusted separately for excitatory and inhibitory CRFs. Fitted model parameters were: $A_e = 99$, $A_i = 9$, $e = 1.2$, $i = 2.5$, $c_{50e} = 0.09$, $c_{50i} = 0.28$, $\alpha = 0.24°$, and $\beta = 6.0°$.

Size Model (Fig. 1): The shape (n and c_{50}) of the CRF was same for excitation and inhibition. Maximum amplitudes (A_e, A_i) were adjusted separately. The size of the excitatory center ($\alpha(c)$) was allowed to vary with contrast and was modeled by a decreasing logistic function (parameters S, m, and k). Fitted model parameters were: $A_e = 51$, $A_i = 0.051$, $n = 1.5$, $c_{50} = 0.04$, $\beta = 2.5°$, $S = 1.0°$, $m = 6.8$, and $k = 0.21$.

Drive Model (Fig. 3B): The shape (n and c_{50}) of the CRF was the same for excitation and inhibition. Maximum amplitudes (A_e, A_i) were adjusted separately. Excitation and inhibition were modeled as in the *CRF Model*, but the excitatory drive (i.e., center activation relative to the maximum center activation: D; $0 < D < 1$) controlled the actual inhibitory influence ($I \cdot D$). D was modeled by an increasing logistic function (parameters m and k). Note that $E_{\max} = ECrf\,(\max(c)) \cdot \max(\mathrm{erf}(w/\alpha)) = ECrf\,(1)$. Fitted model parameters were: $A_e = 97$, $A_i = 0.96$, $n = 1.7$, $c_{50} = .021$, $\alpha = 0.93°$, $\beta = 1.03°$, $m = 1.87$, and $k = 0.19$. Note that spatial extent of inhibition (β) is only about 10% larger than the excitatory center size (α), which is unrealistic in relation to published neurophysiological results (e.g., Allman et al., 1985; Sceniak et al., 1999). When β was constrained to be bigger than 2°, the model fitted data poorly.

We also examined the combination of the *CRF Model* and the *Drive Model* (i.e., by adding parameters i and c_{50i} to the *Drive Model*). This hybrid model yielded an enhanced fit ($df = 20$, $\chi^2 = 10.4$, $p > 0.96$); effectively improving the *Drive Model* fits to data for large sizes.

References

Allman, J., Meizin, F., & McGuiness, E. (1985). Direction- and velocity-specific responses from beyond the classical receptive field in the middle temporal visual area (MT). *Perception, 14*, 105–126.

Anderson, S. J., & Burr, D. C. (1987). Receptive field size of human motion detection units. *Vision Research, 27*, 621–635.

Anderson, S. J., & Burr, D. C. (1991). Spatial summation properties of directionally sensitive mechanisms in human vision. *Journal of the Optical Society of America A, 8*, 1330–1339.

Brainard, D. H. (1997). The psychophysics toolbox. *Spatial Vision, 10*, 433–436.

Cavanaugh, J. R., Bair, W., & Movshon, J. A. (2002). Nature and interaction of signals from the receptive field center and surround in macaque V1 neurons. *Journal of Neurophysiology, 88*, 2530–2546.

DeAngelis, G. C., & Uka, T. (2003). Coding of horizontal disparity and velocity by MT neurons in the alert macaque. *Journal of Neurophysiology, 89*, 1094–1111.

Dragoi, V., & Sur, M. (2000). Dynamic properties of recurrent inhibition in primary visual cortex: contrast and orientation dependence of contextual effects. *Journal of Neurophysiology, 83*, 1019–1030.

Fredericksen, R. E., Verstraten, F. A., & van de Grind, W. A. (1994). Spatial summation and its interaction with the temporal integration mechanism in human motion perception. *Vision Research, 34*, 3171–3188.

Gold, J. I., & Shadlen, M. N. (2000). Representation of a perceptual decision in developing oculomotor commands. *Nature, 404*, 390–394.

Gorea, A. (1985). Spatial integration characteristics in motion detection and direction identification. *Spatial Vision, 1*, 85–102.

Ito, M., & Gilbert, C. D. (1999). Attention modulates contextual influences in the primary visual cortex of alert monkeys. *Neuron, 22*, 593–604.

Kapadia, M. K., Westheimer, G., & Gilbert, C. D. (1999). Dynamics of spatial summation in primary visual cortex of alert monkeys. *Proceedings of the National Academy of Sciences of the USA, 96*, 12073–12078.

Lamme, V. A. (1995). The neurophysiology of figure-ground segregation in primary visual cortex. *Journal of Neuroscience, 15*, 1605–1615.

Lappin, J. S., & Bell, H. H. (1976). The detection of coherence in moving random-dot patterns. *Vision Research, 16*, 161–168.

Levitt, J. B., & Lund, J. S. (1997). Contrast dependence of contextual effects in primate visual cortex. *Nature, 387*, 73–76.

Pack, C. C., Hunter, J. N., & Born, R. T. (2005). Contrast dependence of suppressive influences in cortical area MT of alert macaque. *Journal of Neurophysiology, 93*, 1809–1815.

Pelli, D. G. (1997). The VideoToolbox software for visual psychophysics: transforming numbers into movies. *Spatial Vision, 10*, 437–442.

Roitman, J. D., & Shadlen, M. N. (2002). Response of neurons in the lateral intraparietal area during a combined visual discrimination reaction time task. *Journal of Neuroscience, 22*, 9475–9489.

Sceniak, M. P., Ringach, D. L., Hawken, M. J., & Shapley, R. (1999). Contrast's effect on spatial summation by macaque V1 neurons. *Nature Neuroscience, 2*, 733–739.

Sclar, G., Maunsell, J. H., & Lennie, P. (1990). Coding of image contrast in central visual pathways of the macaque monkey. *Vision Research, 30*, 1–10.

Solomon, S. G., Peirce, J. W., & Lennie, P. (2004). The impact of suppressive surrounds on chromatic properties of cortical neurons. *Journal of Neuroscience, 24*, 148–160.

Somers, D. C., Todorov, E. V., Siapas, A. G., Toth, L. J., Kim, D. S., & Sur, M. (1998). A local circuit approach to understanding integration of long-range inputs in primary visual cortex. *Cerebral Cortex, 8*, 204–217.

Tadin, D., Lappin, J. S., Gilroy, L. A., & Blake, R. (2003). Perceptual consequences of centre-surround antagonism in visual motion processing. *Nature, 424*, 312–315.

Treue, S. (2001). Neural correlates of attention in primate visual cortex. *Trends in Neurosciences, 24*, 295–300.

van de Grind, W. A., Koenderink, J. J., & van Doorn, A. J. (1986). The distribution of human motion detector properties in the monocular visual field. *Vision Research, 26*, 797–810.

Watson, A. B., & Turano, K. (1995). The optimal motion stimulus. *Vision Research, 35*, 325–336.